Volume 1 | Number 1 | Jan 2013 | Pages 1–100

Journal of
Materials Chemistry A

Materials for energy and sustainability
www.rsc.org/materialsA

ROYAL SOCIETY OF CHEMISTRY

www.rsc.org/materialsA

Journal Name

ARTICLE TYPE

Towards industrialization of polymer solar cells: material processing for upscaling

Ignasi Burgués-Ceballos,[a,b] Marco Stella,[a] Paul Lacharmoise[a] and Eugenia Martinez-Ferrero[*a]

In this review, we describe insights into the key aspects of material processing for the industrialization of organic solar cells using printing solutions. The manuscript details the adjustments found in the literature about ink formulation and deposition parameters required to scale up the model system based on P3HT:PC$_{60}$BM, from spin coating to doctor blade or inkjet printing and finally to roll-to-roll deposition.
10 We analyze the particular problems associated to each technique in combination with the common problems linked to the choice of the procedure like the material consumption, the presence of inhomogeneities or time expenses. Moreover, we highlight the use of non-hazardous chemicals and the achievements done in upscaling technology which is nowadays a major topic to construct affordable light conversion devices.

15 Introduction

Since the discovery of light-to-electricity conversion in organic diodes in 1986, there has been an exponential increase in the number of publications and patents in the field of organic solar cells (OSC).[1] This promising technology, in particular polymer
20 solar cells, holds the promise for light weight, flexibility and low cost manufactured devices for the autonomous generation of light, with reported power conversion efficiencies (PCE) of up to 11% and estimated energy payback times (EPBT) of 1.3 years.[2–4] In addition, the processability of the materials in solution paves
25 the way to high throughput production of large area devices that would contribute to the commercial exploitation of the technology and the reduction of the EPBT. However its potential as renewable source of energy has not been fully exploited because research has been mainly focused on chasing higher
30 efficiencies through the design of new materials and photoactive polymers with tuned properties.[5,6] Meanwhile, other crucial aspects remain unattended like the need to replace deposition under inert atmosphere or the use of costly materials. Consequently, the perspectives of mass production decrease when
35 considering that, in addition, the cells are usually designed as non-inverted structures with active layers below 1 cm^2. First of all, it is worth noticing that the lifetime of the conventional structure (namely ITO/hole transport layer, HTL/photoactive layer/ electron transport layer, ETL/ electrode, Figure 1) is
40 compromised by faster degradation. This is due to the use of air sensitive materials for the ETL (Ca or LiF) and the electrode (Al) in contrast to those used in the inverted structure (ITO/ETL/photoactive layer/HTL/electrode), such as silver, and the elimination of the oxygen-sensitive ITO/PEDOT:PSS
45 interface.[7] Second, the power conversion efficiency depends on the size of the active area because of augmented electrical resistive losses and defects when the size is increased.[8] Finally,

there is an impressive number of papers dealing with similar materials but reporting their particular synthetic conditions,
50 which impedes the establishment of clear and reproducible trends. We need to take into account that the performance of the device is intimately related to segregation, crystallinity and topology of the active layer because charge mobility and exciton separation depend on the size of the domains.[9] The resulting
55 morphology is influenced by the solvent nature, the solubility of the reactants and the thermodynamics of the solution which is also affected by the use of additives.[6] Therefore, ink formulation and solution ageing are critical for achieving high efficiencies.[10] For all these reasons, the process of upscaling the so-called lab
60 cells into modules of commercial interest is not straightforward, and consequently, it is not surprising that up to now only prototypes have been manufactured.[11,12]

The most viable approach to large area modules with commercial interest is by printing techniques, which make use of
65 solutions that can be deposited under open air. This strategy allows for low production cost by saving time and energy in the manufacturing process. However, this involves the reformulation of the inks previously tested in smaller lab devices in order to match the technical requirements of the equipment. Additional
70 tests to control the morphology and optimize the thickness and curing conditions are required. On the other hand, the material processing usually involves the use of high boiling point solvents, normally halogenated like dichlorobenzene, to allow for a slow drying process that favours an effective morphology of the
75 layers.[13] These hazardous solvents, which present safety and environmental concerns, are to be banned in the near future for industrial applications and their substitution requires additional research to find the most suitable conditions for device manufacturing, such as solubility, wettability or solution
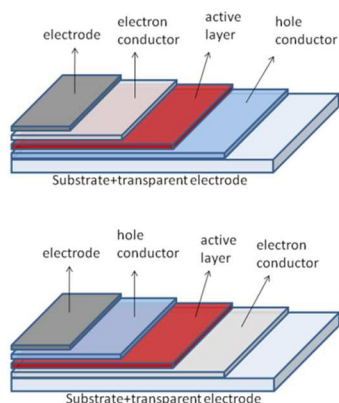80 aggregation.[6,14–16] Therefore, research on both green chemistry

Fig. 1 Conventional (up) and inverted (bottom) structures of OSC.

and deposition should be associated when dealing with upscaling.

In this feature article, we highlight the efforts required to adapt the processing of lab scale devices into pre-industrialized prototypes. We analyze the most common techniques found in the literature for upscaling, namely inkjet printing, doctor blade, slot die and screen printing, and how the inks need to be reformulated to meet their requirements. For this, we use as a model the workhorse system made of PET/ITO/ZnO/P3HT:PCBM/PEDOT:PSS/Ag [where P3HT: poly(3-hexylthiophene); PCBM: (6,6)-phenyl-C_{61}-butyric acid methyl ester] due to its popularity among the research community and the excellent ratio between cost and performance of its constituent materials.[10] Finally, we have added a practical demonstration at the end of the review article describing how to design and estimate the cost of an upscaling experiment.

The system made of PET/ITO/ZnO/P3HT:PCBM/PEDOT:PSS/Ag

The highest reported efficiency for P3HT:PCBM based organic solar cells is 5.16 % which is lower than the highest reported efficiency for polymer solar cells, 9.2 % for PTB7:PC_{71}BM, or even the 8.62% reported for P3HT:ICBA [where PTB7: thieno (3,4-b) thiophene/benzodithiophene; PC_{71}BM: (6,6)-phenyl-C_{71}-butyric acid methyl ester; ICBA: indene C_{60} bisadduct].[17–19] However, the combination of P3HT:PCBM has become the most popular choice among the researchers.[10] The reasons for this are the high charge mobility of the light absorbing P3HT together with the very efficient exciton dissociation that takes place at the P3HT:PCBM interface, where P3HT acts as electron donor and PCBM is the electron acceptor. The benefits of using P3HT rely on its good processability compared to other semiconducting polymers since it can be processed from a myriad of organic solvents using different printing and coating techniques. Moreover, this polymer can be processed in open atmosphere, being thus compatible with roll-to-roll deposition. Finally, it is worth mentioning that due to the widespread use of this material it can be easily acquired in large quantities from different suppliers. Consequently, the price has been constantly decreasing, converting this polymer in the most convenient cost effective option. Regarding the PCBM, current prices of fullerene derivatives make it the most reasonable choice for cost-effective printed devices, although its price is higher than P3HT since its

synthesis requires multiple purification steps. Moreover, the alternatives for well-performing materials are, in this case, fewer.[20] Although new semiconducting polymers have constantly raised the efficiencies of organic solar cells during the last decade, these low band gap polymers are often very unstable and in most of the cases require processing under inert atmosphere. Moreover, their sophisticated synthesis prevents their availability at affordable prices; consequently, these high performing semiconductors have been restricted to lab scale devices processed under strict conditions.

Regarding the architecture of the solar cells, there are four examples of polymer solar cells reported in the literature. The configurations differ in the illumination side, which can be front or back with respect to the substrate, and the electron flow sense, i.e. from the active layer to the front or back electrode. As mentioned before, most of the OPV research is based in square mm-scale devices in which the layers are processed by spin coating, the top electrode is thermally evaporated and the device is encapsulated and characterized in inert atmosphere. Front-side normal geometries are usually chosen in these cases because of the straightforward coating processing of the successive layers. In this case the light enters the cell through the substrate on top of which a transparent electrode is deposited, followed by the high work function hole transport layer and the active layer. Finally the top electrode, made of low work function materials such as LiF/Al or Ca/Al, is smoothly evaporated on top of the active layer (see Figure 1 up). This geometry has been optimized along the years by adding extra functional layers and has become the geometry of choice for testing new materials and device geometries. However, the thermally evaporated electrodes are highly sensitive to oxygen and moisture, thus preventing deposition in open environments. So the search for enhanced lifetimes using air stable electrodes promoted the apparition of the so-called inverted geometry with the resulting structure substrate/cathode/ETL/active layer/HTL/top electrode (see Figure 1 bottom).

Normal geometry devices do not necessarily count with an electron transport layer. The negative charges can be directly extracted from the active layer to the top electrode. However, this presents two main drawbacks. In the first place, the top electrode must be deposited by thermal evaporation since a printed electrode could damage the active layer by solvent diffusion. In the second place, the low work function of the electron collecting top electrode makes it much more reactive to oxidization, thus reducing the stability of the whole device. This reinforces the choice of the inverted geometry for fully printed large area solar cells. In this geometry, the electron transport layer is sandwiched between the bottom electrode and the active layer and must be transparent, reducing the possible material choice. Metal oxides exhibit the best electron transport vs. transparency compromise and are usually processed from nano-particle dispersions. ZnO and Al-doped ZnO are, together with TiO_2, the most widely used materials in the form of nanoparticle dispersions due to their simple synthesis routes and high electron transport through thin transparent layers.[21]

The conducting polymer poly(3,4-ethylenedioxythiophene) (PEDOT) is today the most used hole transport layer for organic solar cells due to its high charge transport rate and optical

transparency.[22] Combined with the solubilizer poly(styrenesulfonate) (PSS), PEDOT is commercially available in the form of inks for spin coating, inkjet and even screen printing. Alternative versions of PEDOT can also be thermally evaporated. Apart from transporting holes and blocking electrons in solar cells architectures, the PEDOT layer is used to smooth the ITO surface in normal geometries and to protect the active layer from the printed metallic electrode in inverted structures. On the other hand, the selection of the metallic electrode depends upon its stability in air and solution processability. In this respect, the most appropriate inks are those based on metallic nanoparticles that maintain their conducting properties upon contact with air, such as those made of silver or copper.

The preferred substrate to manufacture flexible solar cells is made of PET [poly(ethylene terephthalate)] due to its thermal and mechanical resistance combined with a low price, although examples on different plastic substrates such as PEN [poly(ethylene-2,6-naphthalene dicarboxylate] have been reported.[23,24] Indium-doped Tin Oxide (ITO) is usually sputtered on top of the substrate leaving a relatively flat surface for subsequent homogeneous thin film coating. This metal oxide has been widely used as a transparent electrode due to its excellent properties, mainly its high stability and good compromise between transparency (~90 %) and conductivity (sheet resistance of 8-12 Ω/sq). However, the high energy consumption required during sputtering and patterning of the ITO electrode and the low abundance of the Indium element in Earth's crust make ITO a major contributor to the module cost as well as to the module embedded energy. Additionally, the use of ITO in flexible devices may not be recommended due to possible cracking or delamination and conductivity losses with bending. Therefore, there is an intensive research for alternative cost-effective material with high conductivity, transparency and flexibility.[25]

Particular conditions of different techniques

Inkjet printing

Besides traditional graphical printing techniques, inkjet printing (IJP) has been used in the last few years as a fabrication tool in advanced areas of technology. This technique has been applied in the construction of devices like thin film transistors, light emitting diodes, memory devices, organic solar cells, conductive structures, sensors and biological applications.[26]

Inkjet printing allows the deposition of thin films (from nanometers to microns) from dissolved or dispersed materials on any substrate in a reproducible manner. The extremely accurate positioning of individual picolitre droplets that are ejected from piezoelectric-controlled nozzles represents an advantage that allows for direct digital patterning, which in turn leads to efficient material-saving avoiding the use of expensive masks. Moreover, contamination is minimized because inkjet printing is a non-contact deposition method. A typical lateral resolution in the micrometer scale can be achieved by using lab-scale printers. The processing speed depends on the number of printing jets. Currently, commercially available tools can simultaneously use up to 1024 jets, which enable printing at speeds of 500 mm/s.[27] Furthermore, the compatibility of inkjet printing with reel-to-reel (R2R) processes makes it industrially relevant.
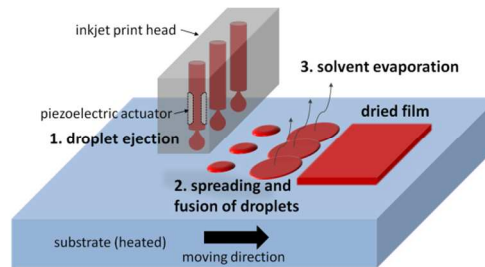

Fig. 2 Operating principle of a drop-on-demand inkjet printing system.

The working principle consists in three steps: (i) droplet formation and ejection, (ii) positioning, spreading and coalescence of droplets on a surface and (iii) solvent evaporation and other mechanisms that result in a dried, solid film (Figure 2). The reader is referred to recent reviews for a complete description of the printing mechanism.[28,29] On the other hand, inkjet printing is considered a slow drying technique, in contrast to faster drying processes such as spin coating. This, together with the difficulty to control all the processing parameters, has been a constraint for a wide spreading of this processing tool. A deep understanding of the technique itself as well as of the parameters affecting the drying behaviour is mandatory to achieve homogeneous layers, even more when specific layer morphology is sought, as in the case of the active layer in organic solar cells. Unlike other robust printing methods like screen printing or slot die, inkjet printing requires specific ink properties such as viscosity, surface tensions or solvent composition, which can influence both deposition and film formation. In this sense, a typical problem related to solvent composition is the so-called c*offee stain effect*, a migration of the deposited material to the edges of the printed pattern during film formation, especially with long drying times. This is due to a combination of contact line pinning of the droplet and faster solvent drying at the edges, which creates a gradient of concentration and a subsequent liquid flow.[30] This feature can be suppressed, for example, through an adequate design of solvent mixtures, as proposed by de Gans et al. who showed how a mixture of high boiling point, low surface tension solvent with a low boiling point, high surface tension solvent leads to increased film homogeneity. The migration of the material is mitigated by the Marangoni flow due to the new gradient of surface tension that appears in the opposite direction of the concentration gradient.[31] Since printing parameters have also an enormous influence on all these aspects, they can be carefully used to adapt or compensate ink characteristics.

In the OPV field, relevant improvements have been achieved in the last 6-7 years. Interestingly, examples of standard structured solar cells with selective inkjet printed layers can be found in literature. For instance, the formulation of an ITO nanoparticle-based ink has been reported.[32] Alternatively, relevant results in ITO-free devices based on inkjet printed current collecting grids made of silver inks have also been published. Galagan and coworkers inkjet printed both silver grids and PEDOT:PSS layers obtaining efficiencies of 1.54 % with an impressive area of 4 cm^2.[33] Other works, focused on PEDOT:PSS layers, include a comparative study between spin coating, spray coating and inkjet printing or the optimization of the PEDOT:PSS ink formulation by using solvent additives.[34,35] Finally, top electrodes have been printed as well using metallic nanoparticle

inks.[36] However, the main research interest has been focused on the photoactive layer through the investigation of the effects that particular parameters have on OSC performance. The concentration of the semiconductor blend has been related to surface roughness by Aernouts et al. who reported that higher blend concentrations tend to give rougher layers.[37] High boiling point solvents induce, on the other hand, higher roughness in inkjet printed layers too.[38] Moreover, the influence of the solvent composition in the drying process and the morphology of the film has been determined by mixing high and low boiling point solvents, like o-dichlorobenzene/mesitylene, which resulted in a twofold increase of efficiency when compared to pristine tetralin.[39] On the other hand, a multiparametric study has identified some of the critical parameters and the crossed relationships between viscosity, temperature of the substrate, drop spacing and the height between nozzle and substrate.[40] Another relevant approach has used inkjet printing for combinatorial screening of polymer:fullerene blends with low material investment.[41]

The best OPV performance reported up to now with inkjet printed P3HT:PCBM layers was achieved by Eom et al. with the addition of 1,8-octanedithiol as a high boiling point additive (PCE = 3.71%).[42] This work, as well as the one reported by Lange et al., have the extra merit of including inkjet printed PEDOT:PSS.[43] From these data, we infer that a careful study of ink formulation and printing conditions is essential to obtain homogeneous films with adequate morphology for best OPV performance. In addition, physical properties such as the contact angle between the solution and the substrate need to be controlled to ensure optimal wetting.

Table 1 shows a selection of the most representative results.

Table 1. Performance of selected OSC based on P3HT:PCBM devices with conventional structure with at least one layer processed by inkjet printing.

Inkjet printed layer	Solvent[a]	η /%	Area /cm²	Ref.
1 inkjet printed layer				
ITO	EtOH	1.8	0.0625	32
Ag[b]		1.96	0.09	44
PEDOT:PSS		3.31	NA	34
P3HT:PCBM	DCB:MES	3.47	0.2-1	39
Ag[d]		1.96	1	36
2 inkjet printed layers				
Ag[b]/**PEDOT:PSS**		1.54	4	33
Ag,[b] **P3HT:PCBM**	DCB:MES[c]	2.54	0.25	45
PEDOT:PSS/P3HT:PCBM	CB:ODT[c]	3.71	0.09	42

[a] Used in the inkjet printing step. Commercial inks when not specified. MES:mesitylene; [b] bottom electrode; [c] for the active layer; [d] top electrode

Table 2 shows a general overview of the interplay of all the parameters involved in inkjet printing. The considered parameters are classified as ink, substrate or inkjet printer dependent, and correlated to different aspects of the processing steps. Although this multi-parametric puzzle evidences that a deep control of inkjet printing process is not trivial, the results obtained so far are encouraging. Moreover, according to all these reports, there are

Table 2 Crossed interactions between processing parameters (rows) and the effects within the inkjet printing process (columns). Filled symbols indicate strong interactions while empty marks point to weak relations.

		Ejection					Spreading		Drying	Film formation				
		nozzle clogging	jetability	drop shape	volume	speed	drop diameter	coalescence	time	resolution	thickness	roughness	depth composition	lateral homogeneity
Ink	solid content	○	○	○							●	●		
	solvent composition	●	●				○	○	●	○		○	●	●
	viscosity		●	●		○	●	○						●
	surface tension		●	●		○	●	●		○				●
	vapour pressure	●	●						●			○		
Substrate	surface properties						●	●		○			●	●
	temperature						○	○	●	○			●	●
IJP parameters	nozzle diameter	○	○		●		●	○	●					
	cartridge temperature	●	●	○		○	○	○						
	piezo waveform		●	●	○	○	○	○		○	○			
	firing voltage		○		●	●	○	○		○	○			
	printhead height						○	○		○				
	number of jets							●	●				○	○
	drop spacing						●	●			●	○		●

Journal Name

Dynamic Article Links ▶

ARTICLE TYPE

not fundamental limitations to implement inkjet printing for processing all the layers to construct OPV devices. Indeed, there are two recent examples of solar cells fully processed by inkjet printing.[46,47] In the case of the Solliance consortium, the authors
5 claim that the six-layer stack, ITO-free solar cell were produced at R2R compatible speeds. In line with this, a remarkable inkjet printing integration into a roll-to-roll equipment has been used by Angmo et al. to produce silver grids as electrodes for ITO-free devices.[36] It is thus clear that inkjet printing is attracting more and
10 more interest as an OPV production tool.

Doctor Blade

In the case of doctor blade, the ink is deposited onto the substrate by means of a coating knife that is placed at a fixed distance from the surface. The blade moves linearly over the substrate at a
15 constant velocity, spreading the ink and producing a wet film which dries due to the solvent evaporation (Figure 3). The film is then the result of the combination of ink properties and blading parameters. Therefore, film roughness and morphology, surface wettability, and the coverage of the substrate are determined by
20 the solution and the substrate properties together with the distance between substrate and blade, its speed and the temperature of the substrate. The crossed interactions between all the parameters involved in the process are shown in Table 3. Typical speeds range between 1 and 15 mm/s producing films in
25 the submillimetric scale from ten to hundreds of nanometers. The ideal thickness of the layer depends on its function; therefore, charge transport layers must be thin enough to have satisfactory mobility values while thick enough to avoid pinholes whereas the active layer must maximize light absorption and carrier
30 generation and transport.

Doctor blade is a facile method to enlarge the active area of the devices with low material waste. In fact, it is easily transferable to a reel-to-reel system where it is known as knife-over-edge coating. In this case, the knife is fixed and the rolled substrate
35 moves. However, it does not allow for patterning and the viscosity of the ink must be high enough to avoid leaking or running back on the roll (suitable values should range between 100 and 20000 mPa·s). Therefore, with such requirements this technique has been rarely used in the production of solar
40 cells.[48,49]

Although it is an easily available technique, doctor blading has been relegated by spin coating as the technique of choice for building lab-scale devices. Few approaches have been made during the past decade to explore the fabrication of large area
45 devices and modules on flexible substrates.[50–52] More recently, the effect of additives and the resulting morphology of the films deposited by doctor blade has been exhaustively studied.[53–55] Compared to spin coating, doctor bladed films offer large-area uniformity and more control of the orientation of the films. For
50 example, slow drying at low temperatures favours strong P3HT π-π ordering along the substrate surface (the so-called edge-on orientation) that has been
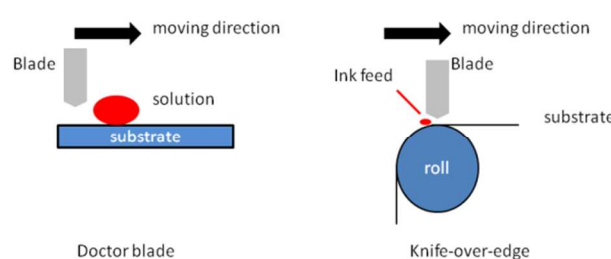
Fig. 3 Schematic representation of the coating techniques of doctor blade
55 and knife-over-edge coating.

proved to give the best device performance. Moreover, the coating quality obtained by doctor blade is best at 15ºC because of the higher viscosity that suppresses dewetting effects.[55] On the other hand, the comparison between spin coating and doctor
60 blade indicates that the devices prepared by doctor blade show higher efficiencies due to increased photocurrent and V_{oc} originated by slightly thicker films and enhanced quality of the different interfaces.[50,56] A plausible explanation is that doctor blading promotes slower solvent evaporation which in turn
65 favours molecular self-organization while preventing interlayer dissolution.[57]

Table 3 Crossed interactions between the doctor blade processing parameters (rows) and the effects within the printing process (columns). Filled symbols indicate strong interactions while empty marks point to
70 weak relations.

		Spread		Dry	Film formation			
		Surface coverage	Surface wettability	time	morphology	thickness	roughness	homogeneity
Ink	solid content				●	●	●	○
	solvent composition	○	●	●	●			○
	viscosity	●	●		○		○	
	surface tension	●	●	○				
	vapour pressure			●	●		○	
	volume	●				○		
Substrate	surface properties	●	●		○		●	
	temperature	○	●	●	●		○	
Blade	blade height	●				●	●	●
	blade speed	○	○	○		●	●	●

Blading has also been specifically applied to print the charge transport layers on devices where the active layer is deposited by other techniques. There are examples of films made of PEDOT:PSS and homogeneous layers of silver nanowires and
75 silver grids that have been prepared to replace the ITO

layer.[58,59,38] However, patterning is difficult and therefore all the papers consulted report deposition of the metallic counterlectrodes by vacuum thermal evaporation. In this sense, the efforts done in the construction of organic thin film transistors
5 for patterning doctor-bladed films through photolithography, prepatterning of the substrates and subsequent control of the surface tension gradient of the ink should be mentioned.[60]

Therefore, although being less popular than spin coating, the doctor blade technique permits more control over the film
10 morphology and an easier transition to R2R. Optimized P3HT:PCBM-based devices have shown efficiencies higher than 4%.[50] The benefits of the doctor blade technique have recently crystallized in the construction of tandem cells due to the possibility to work on large areas in air with commercial
15 materials.[61,62] This boost has been favoured by the intensive development of solution processed intermediate layers like ZnO, TiO_x or PEDOT:PSS that allow for low annealing temperatures compatible with the previously deposited bottom cell.[63] Although the use of P3HT:PCBM in multijunction devices limits the
20 efficiency due to their low V_{oc}, record values of 4.85% have been obtained when combining P3HT:PCBM with Si-PCPDTBT:PCBM.[61]

Finally, it is worth mentioning that excellent efficiencies of 4% have been obtained by different teams without making use of
25 halogenated solvents.[50,57]

Slot Die

The slot die technique makes use of a stainless steel printing head fed with an ink which is flown using a proper pumping system. The ink goes through a slot, which width is defined by a mask
30 which separates the two head components, and falls onto the substrate (Figure 4). This system can be applied both to discrete sheet-to-sheet and continuous roll-to-roll systems. In the latter case, large surface printing and upscaling processing are possible since web speeds of several m·min^{-1} are allowed being the only
35 limitation the fact that coating becomes unstable at high speeds.[64] Moreover, slot die allows direct patterning in form of stripes by employing masks with free regions where the ink can flow (Fig. 5). The mask plays a major role since its thickness can vary in the range of tens of microns depending on ink viscosity which can
40 range between a few mPa·s and hundreds mPa·s. One important aspect to consider is that thin masks are more prone to deform during its handling and the mask status degradation can lead to undesired effects on the printing process. Moreover, the mask has to be designed and produced for each new pattern. Another
45 component that is strongly conditioned by the rheological properties of the ink is the pumping system. Peristaltic and piston pumps are suitable for low viscosity inks like those made of P3HT:PCBM and ZnO, while pressure tank pumps are used for viscous pastes. Three additional crucial aspects to take into
50 account are: (i) the maintenance of the pressure of the printing head to avoid pressure leaks and subsequent thickness variations between stripes; (ii) the compatibility between solvents and the printing systems to avoid possible chemical contaminations, and (iii) film registration to ensure that each layer is well positioned
55 with respect to the others since accurate positioning has an important influence when fabricating modules if the active area is to be maximized.
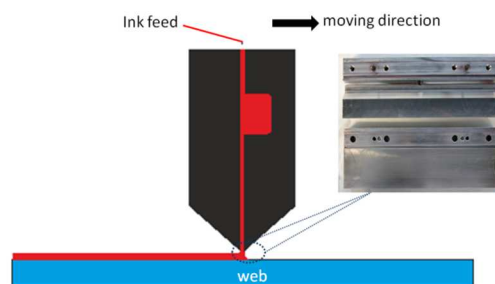

60 **Fig. 4** Scheme of the slot die printing head depositing a curtain of ink showing the slot die printing head from inside.

Regarding the printing of inverted solar cells, and opposite to the other techniques showed before, slot die can be used for all the layers, except for the silver top electrode which is usually printed
65 by screen printing (*vide infra*).[65] The PEDOT:PSS can alternatively be deposited by screen printing as well. The so-defined slot die/screen printing process can be applied both to sheet-to-sheet and roll-to-roll systems and has been proven as a good upscale model for OPV industrialization.[66] The optimization
70 of the process involves many parameters related to the printing system, such as web speed, ink flow and oven length, and parameters related to the ink formulation, like the solvent type and solid concentration. The combination of both, described in Table 4, determines the resulting thickness and the nano and
75 macro-morphology quality of the deposited material.

Table 4 Crossed interactions between processing parameters (rows) and the effects within the slot die printing process (columns). Filled symbols indicate strong interactions while empty marks point to weak relations.

		Ink flow		Dry	Film formation				
		complete pattern	volume	time	resolution	thickness	roughness	depth composition	lateral homogeneity
Ink	solid content			●		●	●		○
	solvent composition	○		●	○		○	●	●
	viscosity	●	●						●
	surface tension				●				●
Substrate	surface properties	○			●		○		●
	web speed	○		○	○	●			○
Slot die	mask thickness	○	●				●		
	pumping system	●	●				●		○

Given an ink formulation, the flow, defined through the pumping
80 system, determines the amount of ink to be deposited on the substrate and, as a consequence, the dried film thickness. Nevertheless, a weak flow does not guarantee homogeneous printing from all the printing head slits when using viscous inks. On the contrary, a high flow could result in the loss of pattern
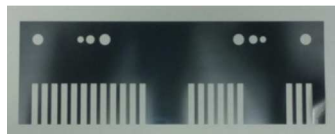85 resolution giving rise to stripes 10% wider than the nominal width.

Fig. 5 Picture of the mask used to print stripes.

Furthermore, since the drying kinetics determine the layer morphology at both the macro and nanoscale, the amount of deposited ink and the drying time must be correlated. The web speed can be tuned, in combination with the ink flow, to determine the film thickness and, thus, the quicker the substrate moves, less material is deposited on it. In turn, the web speed also influences the time that the material transits the oven and, consequently, the curing time. Oven length is a fixed parameter for each roll-to-roll machine and must always be taken into account when choosing the deposition parameters because of the influence that curing time has on the active layer nano-morphology and cell performance.[13]

The choice of concentration and solvent type of the ink influences film thickness and morphology. The inks employed for organic solar cells have a solid content between 1% and 5% resulting in thicknesses ranging between tens of nanometers and few microns. ZnO can be printed using nanoparticle dispersions in solvents like methanol, acetone or chlorobenzene with concentrations of tens of mg·ml^{-1}.[67] In this case thicknesses between 10 and 100 nm can be deposited with concentrations between 2% and 5% using a peristaltic pump. An important factor to be considered is the solvent evaporation rate since fast solvent removal could cause slot obstruction and ink flow instability while slow evaporation rates promote solid agglomeration in the wet film during the drying process. On the other hand, the ink solvent can interact with the equipment as it is shown in Figure 6. Both films on Figure 6a and 6b have been deposited from inks containing methanol but making use of different tubes. The film on Fig 6a is affected by the release of additives from the tube into the ink which results in the formation of pinholes, while the film on Figure 6b possesses a better morphology. Regarding the P3HT:PCBM solution, the solvents of choice must have lower boiling points than those used for spin coating. This is done to have faster drying rates, even if a post-deposition annealing is required to improve the material nano-morphology. In addition, the solution of the mixed precursors is left several hours prior to printing to favour the mixture. Nevertheless, macroscopic defects can still be observed by naked eye in certain deposition conditions, especially with higher volumes. Figures 6c and 6d illustrate the difference between two films prepared from inks with different solid content. The variation from 2.4% wt to 4.8% wt results in film thicknesses of approximately 200 nm and 400 nm, respectively. As it can be seen in Figure 6c, the film obtained from the less concentrated solution is affected by inhomogeneities formed during the drying step, indicated by the yellow arrows. The second film, Figure 6d, is not affected by such defects due to the slightly lower solvent content and higher viscosity. Finally, the need to ensure the security of the R2R operators through the reduction of damage due to solvent exposure has promoted the research on roll-to-roll printed non-harmful inks for application in OPV.[68,69]
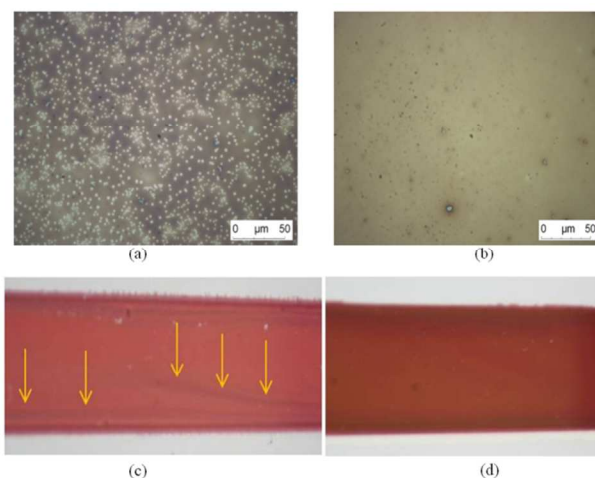

Fig. 6 Micrographs of ZnO films (a) affected by pin holes compared to homogeneous films (b); P3HT:PCBM samples deposited by slot die. Film 6c has been deposited from a less concentrated solution (defects highlighted by yellow arrows) while film 6d has been deposited from a more concentrated solution.

Screen printing

Screen printing is a traditional printing technique which allows 2D patterning and can be employed for both sheet-to-sheet and roll-to-roll systems. The most important characteristic of such technique is that inks must have viscosities in the order of Pa·s, which are not compatible with many of the inks used for OPV. Nevertheless, screen printing is an essential tool in some of the industrial processes currently used to fabricate inverted OPV modules because PEDOT:PSS and silver can be printed by this technique. The working mechanism is shown in Figure 7 and is based on the use of a textile screen which is previously covered with an UV cured emulsion on the entire surface with the exception of the regions where the pattern must be printed. A certain amount of paste is placed on the screen and a squeegee is used to make it to filter through the screen onto the substrate. The screen printing pastes can be cured by temperature annealing or upon UV exposure. Such technique offers easiness of use and high throughput, being able to be integrated in a roll-to-roll system. Moreover, commercial pastes are easily available at lower prices than those for inkjet printing avoiding an important work of formulation. Regarding the formulation, the viscosity required, between 3 to 20 Pa·s, makes it difficult to print by this method materials like P3HT, PCBM and ZnO. Other crucial aspects related to formulation are the micrometric thickness of the printed layers and the need for solvents with low evaporation rate to avoid material drying in the screen. All these parameters are described in Table 5.

There exist few examples in literature of screen printed OPV modules by using thermocleavable solvents which give the ink enough viscosity and which have low evaporation rates.[70,71] For these reasons, screen printing is more often employed as a complementary printing technique to finish the devices with silver, especially in the case of slot die-based processes.[66]
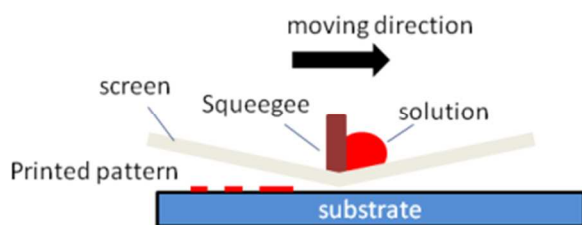
Fig. 7 Schematic illustration of the screen printing technique.

Table 5 Crossed interactions between processing parameters (rows) and the effects within the screen printing process (columns). Filled symbols indicate strong interactions while empty marks point to weak relations.

		Spread		Dry	Film formation			
		complete pattern	volume	time	resolution	thickness	roughness	lateral homogeneity
Ink	solid content			●		●	●	○
	solvent composition			●	○		○	●
	viscosity	●	●		○	○		●
	surface tension				●			●
Substrate	surface properties	●			●		○	●
Screen web	thickness	○	●			●	●	○

Practical example for upscaling: design of an experiment

The main issue to deal with when planning to use the roll-to-roll system is the cost that each experiment requires in both economic and temporal terms. On the other hand, stepping from the most employed deposition technique in laboratory scale, spin coating, to slot die ~~is a process that~~ can imply a huge work of research, due to the important technical differences regarding distribution mechanism on the surface of the substrate and the drying dynamics. As a consequence, ink formulation can imply important differences from one technique to another. In order to develop an industrial process, then, it seems reasonable to directly operate using the same technique as the one to be used in the final industrial process. Slot die is a technique that allows great area deposition in a very short time but roll-to-roll equipment implies very high material cost. Moreover, a roll-to-roll experimental session can be expensive also in terms of time employed to perform all the required characterizations. One way to avoid such problems is to use sheet-to-sheet slot die coating systems which provide the possibility to employ reduced amounts of materials in shorter processing times. Nevertheless, since feasible industrial processes require the use of roll-to-roll systems, it is mandatory to undertake research directly with preindustrial systems based on this concept. In this section, we want to describe an estimation of an experimental session of R2R. It is beyond the scope of this article to provide a detailed

economic assessment or Life Cycle Analysis (LCA) of the modules so we refer the interested readers to articles found in the literature.[4,72] In this sense, we do not consider the barrier material in our assumption, which is a potential source of expenses employed to prevent moisture and oxygen degrading the modules. The encapsulation adds notable variation of prices depending on the chosen approach (polymers or a combination of polymers and nanoparticles). In fact, when doing preliminary tests, as it is the case of this example, it is not worth using efficient but expensive barrier materials, being the simplest option to use pressure sensitive adhesives in combination with PET foil.[72]

The material costs for printing reduced, cost-effective modules of inverted architecture are detailed in Table 6.

Table 6 Detailed cost of the materials required to prepare 1 m^2 modules.

Material	Provider	Amount (unit)	Cost of material (€/unit)	Cost per module (€/m^2)
Patterned PET/ITO	Multek; Mekoprint[a]	1 m^2	89.26	89.26
ZnO dispersion	Synthesized in the lab	0.71 ml	0.47[b]	0.33[b]
P3HT:PCBM ink	Rieke Metals; Solenne BV; Sigma Adrich	1.31 ml / 3.45 ml	13.52 / 13.67	17.71[c] / 47.16[d]
PEDOT:PSS	Agfa	2.86 g	0.98	2.80
Ag	DuPont	2.38 g	1.3	3.09
TOTAL				113.19[c] / 142.64[d]

[a)] The PET/ITO substrate is acquired from Multek and subsequent ITO patterning is done by Mekoprint; [b)] final price considering all the reactants required to synthesize ZnO; [c)] Thickness of the active layer: 150 nm; [d)] Thickness of the active layer: 400 nm

In this case, slot die has been considered for ZnO and P3HT:PCBM and screen printing for PEDOT:PSS and Ag. While the later allows deposition of the material only where it is required, with only a marginal amount of paste wasted on the screen, slot die covers the entire substrate roll with a higher ink waste. For the calculation, electricity, water and personnel are not included, while approximated amounts of materials have been considered based on our experience and the price provided by suppliers. The cost of the substrate includes the proportional amount that remains unused behind and beside the printed module to keep the substrate tightly rolled. Moreover, it must be considered that the amounts of the material and the final cost strongly depend upon the thickness of each layer. For this reason, we provide two different thicknesses of the active layer as an example to show the influence that such a component has on the final cost. It is worth noticing that the prices considered in this article correspond to acquisitions of small quantities, this is, non-industrial amounts. It is clear that most of the expenses are brought by the ITO coated PET substrate and the photoactive P3HT and PCBM polymers, therefore an effective cost reducing policy implies finding alternatives to these two components.

Conclusions and Perspectives

This paper has described the challenges of upscaling solar cells by different printing techniques from the previously acquired

knowledge in smaller devices. With the aim of providing a brief guide, Table 7 contains a comparison of the techniques analyzed in this article in terms of advantages and disadvantages, the viscosity of the inks and the resulting thickness of the layers. A selection of record values of PCE reported so far is also included. Obviously, the selection of a particular technique is determined by the characteristics of the device, so parameters like size, structure, and type of substrate or the speed of deposition must be first taken into account. In a second step, the inks need to be accommodated to the selected technique. Hence, the viscosity and wettability together with the evaporation rate of the solvent and the post deposition conditions need to be adapted. The solid content, solvent nature and the speed of deposition determine the kinetics of drying and the resulting morphology of the film which is one of the key factors governing device performance. At the same time, the ease of use makes doctor blade the technique of choice for fast preparations whereas inkjet printing, screen printing and slot die deposition offer great pattern definition and high throughput.

At this moment, inkjet printing and slot die, complemented by screen printing, are the techniques of choice for OPV upscale production. The current state-of-the-art does not allow envisaging which one will prevail because both techniques are being used by the companies that are currently involved in OPV-module development and production. Inkjet printing is widely used in many industrial applications requiring printed electronics so further development is expected in a short period of time. On the other hand, slot die is the best option when looking for easy-to-use low cost equipment. So the choice is more likely to depend on the previous acquired experience of the specific enterprise.

Table 7 Characteristics of the printing techniques reviewed in this paper. PCE record values at 1000 W/m^2 for printed P3HT:PCBM active layer taken from literature.

Technique	Viscosity	Thickness	Advantages	Disadvantages	PCE (%)
Inkjet printing	mPa·s	nm	Fine Patterning Micrometer resolution 2D patterning Low material waste	Exigent ink formulation Expensive inks Not easy to use	3.7[42]
Doctor blade	mPa·s	nm	Fast Low material waste Easy to use	No patterning	4.1[50]
Slot die	mPa·s	nm/μm	Ink versatility Relative ease of use High throughput	1D patterning	3.1[69,73]
Screen printing	Pa·s	μm	2D Patterning Easy to use	Viscous pastes required	0.2[74]

In any case, it is clear that printing techniques offer a wide array of possibilities to create on-demand OPV and are actively contributing to the development of reliable industrial processes. Therefore, the deployment of the OPV technology is mostly conditioned to the reduction of the cost of the materials, the substitution of hazardous solvents, and the enhancement of the stability and lifetime of the modules. These goals can only be reached with the active participation of all the sectors involved, such as research laboratories, technological developers and industrial manufacturers.

Acknowledgements

Notes and references

^{a} CETEMMSA Technological Centre, Avda. Ernest Lluch 36, E-08302 Mataró, Spain. Fax: 0034 93 741 9228; Tel: 0034 93 741 9100; E-mail: emartinez@cetemmsa.com
^{b}Institut de Ciència de Materials de Barcelona (ICMAB-CSIC), Campus de la UAB, E-08193 Bellaterra, Spain

1. M. Jørgensen, J. E. Carlé, R. R. Søndergaard, M. Lauritzen, N. A. Dagnæs-Hansen, S. L. Byskov, T. R. Andersen, T. T. Larsen-Olsen, A. P. L. Böttiger, B. Andreasen, L. Fu, L. Zuo, Y. Liu, E. Bundgaard, X. Zhan, H. Chen, and F. C. Krebs, *Sol. Energy Mater. Sol. Cells*, 2013, **119**, 84–93.
2. M. A. Green, K. Emery, Y. Hishikawa, W. Warta, and E. D. Dunlop, *Prog. Photovoltaics Res. Appl.*, 2014, **22**, 1–9.
3. G. Li, R. Zhu, and Y. Yang, *Nat. Photonics*, 2012, **6**, 153–161.
4. B. Azzopardi, C. J. M. Emmott, A. Urbina, F. C. Krebs, J. Mutale, and J. Nelson, *Energy Environ. Sci.*, 2011, **4**, 3741.
5. P. M. Beaujuge and J. M. J. Fréchet, *J. Am. Chem. Soc.*, 2011, **133**, 20009–29.
6. Y.-W. Su, S.-C. Lan, and K.-H. Wei, *Mater. Today*, 2012, **15**, 554–562.
7. M. P. de Jong, L. J. van IJzendoorn, and M. J. A. de Voigt, *Appl. Phys. Lett.*, 2000, **77**, 2255–2257.
8. D. Gupta, M. Bag, and K. S. Narayan, *Appl. Phys. Lett.*, 2008, **93**, 163301.
9. Z. Masri, A. Ruseckas, E. V. Emelianova, L. Wang, A. K. Bansal, A. Matheson, H. T. Lemke, M. M. Nielsen, H. Nguyen, O. Coulembier, P. Dubois, D. Beljonne, and I. D. W. Samuel, *Adv. Energy Mater.*, 2013, **3**, 1445–1453.
10. M. T. Dang, L. Hirsch, and G. Wantz, *Adv. Mater.*, 2011, **23**, 3597–3602.
11. J. E. Carlé and F. C. Krebs, *Sol. Energy Mater. Sol. Cells*, 2013, **119**, 309–310.
12. R. Po, A. Bernardi, A. Calabrese, C. Carbonera, G. Corso, and A. Pellegrino, *Energy Environ. Sci.*, 2014, 925–943.
13. G. Li, V. Shrotriya, J. Huang, Y. Yao, T. Moriarty, K. Emery, and Y. Yang, *Nat. Mater.*, 2005, **4**, 864–868.
14. C.-D. Park, T. A. Fleetham, J. Li, and B. D. Vogt, *Org. Electron.*, 2011, **12**, 1465–1470.
15. As an example, Eur. Chem. Regul. can be seen http//www.chemsec.org/what-we-do/sin-list.
16. Y. Chen, S. Zhang, Y. Wu, and J. Hou, *Adv. Mater.*, 2014, **26**, 2744–9.
17. S.-H. Lee, D.-H. Kim, J.-H. Kim, G.-S. Lee, and J.-G. Park, *J. Phys. Chem. C*, 2009, **113**, 21915–21920.
18. Z. He, C. Zhong, S. Su, M. Xu, H. Wu, and Y. Cao, *Nat. Photonics*, 2012, **6**, 593–597.
19. G. Zhao, Y. He, and Y. Li, *Adv. Mater.*, 2010, **22**, 4355–8.
20. T. P. Osedach, T. L. Andrew, and V. Bulović, *Energy Environ. Sci.*, 2013, **6**, 711.
21. S. Chen, J. R. Manders, S.-W. Tsang, and F. So, *J. Mater. Chem.*, 2012, **22**, 24202.
22. Y. Meng, Z. Hu, N. Ai, Z. Jiang, J. Wang, J. Peng, and Y. Cao, *ACS Appl. Mater. Interfaces*, 2014, **6**, 5122–9.
23. X. Zhang, K.-S. Liao, A. Haldar, N. J. Alley, and S. A. Curran, *J. Appl. Phys.*, 2013, **114**, 053103.
24. Y. Jouane, S. Colis, G. Schmerber, A. Dinia, P. Lévêque, T. Heiser, and Y.-A. Chapuis, *Org. Electron.*, 2013, **14**, 1861–1868.
25. K. Ellmer, *Nat. Photonics*, 2012, **6**, 809–817.
26. M. Singh, H. M. Haverinen, P. Dhagat, and G. E. Jabbour, *Adv. Mater.*, 2010, **22**, 673–685.
27. www.ceradrop.fr.
28. E. Tekin, P. J. Smith, and U. S. Schubert, *Soft Matter*, 2008, **4**, 703.

29. B. Derby, *Annu. Rev. Mater. Res.*, 2010, **40**, 395–414.

30. R. D. Deegan, O. Bakajin, T. F. Dupont, G. Huber, S. R. Nagel, and T. A. Witten, *Nature*, 1997, **389**, 827–829.

31. B.-J. de Gans and U. S. Schubert, *Langmuir*, 2004, **20**, 7789–7793.

32. H.-K. Kim, I.-K. You, J. B. Koo, and S.-H. Kim, *Surf. Coatings Technol.*, 2012, **211**, 33–36.

33. Y. Galagan, E. W. C. Coenen, S. Sabik, H. H. Gorter, M. Barink, S. C. Veenstra, J. M. Kroon, R. Andriessen, and P. W. M. Blom, *Sol. Energy Mater. Sol. Cells*, 2012, **104**, 32–38.

34. K. X. Steirer, J. J. Berry, M. O. Reese, M. F. A. M. van Hest, A. Miedaner, M. W. Liberatore, R. T. Collins, and D. S. Ginley, *Thin Solid Films*, 2009, **517**, 2781–2786.

35. S. H. Eom, S. Senthilarasu, P. Uthirakumar, S. C. Yoon, J. Lim, C. Lee, H. S. Lim, J. Lee, and S.-H. Lee, *Org. Electron.*, 2009, **10**, 536–542.

36. D. Angmo, T. T. Larsen-Olsen, M. Jørgensen, R. R. Søndergaard, and F. C. Krebs, *Adv. Energy Mater.*, 2013, **3**, 172–175.

37. T. Aernouts, T. Aleksandrov, C. Girotto, J. Genoe, and J. Poortmans, *Appl. Phys. Lett.*, 2008, **92**, 033306.

38. C. N. Hoth, P. Schilinsky, S. A. Choulis, and C. J. Brabec, *Nano Lett.*, 2008, **8**, 2806–2813.

39. C. N. Hoth, S. A. Choulis, P. Schilinsky, and C. J. Brabec, *Adv. Mater.*, 2007, **19**, 3973–3978.

40. M. Neophytou, W. Cambarau, F. Hermerschmidt, C. Waldauf, C. Christodoulou, R. Pacios, and S. A. Choulis, *Microelectron. Eng.*, 2012, **95**, 102–106.

41. A. Teichler, R. Eckardt, S. Hoeppener, C. Friebe, J. Perelaer, A. Senes, M. Morana, C. J. Brabec, and U. S. Schubert, *Adv. Energy Mater.*, 2011, **1**, 105–114.

42. S. H. Eom, H. Park, S. H. Mujawar, S. C. Yoon, S.-S. Kim, S.-I. Na, S.-J. Kang, D. Khim, D.-Y. Kim, and S.-H. Lee, *Org. Electron.*, 2010, **11**, 1516–1522.

43. A. Lange, M. Wegener, C. Boeffel, B. Fischer, A. Wedel, and D. Neher, *Sol. Energy Mater. Sol. Cells*, 2010, **94**, 1816–1821.

44. M. Neophytou, F. Hermerschmidt, A. Savva, E. Georgiou, and S. A. Choulis, *Appl. Phys. Lett.*, 2012, **101**, 193302.

45. I. Burgués-Ceballos, N. Kehagias, C. M. Sotomayor-Torres, M. Campoy-Quiles, and P. D. Lacharmoise, *Sol. Energy Mater. Sol. Cells*, 2014, **127**, 50–57.

46. S. Jung, A. Soul, K. Banger, D.-H. Ko, P. C. Y. Chow, C. R. McNeill, and H. Sirringhaus, *Adv. Energy Mater.*, 2014, DOI:10.1002/aenm.201400432.

47. www.solliance.eu.

48. F. C. Krebs, *Sol. Energy Mater. Sol. Cells*, 2009, **93**, 465–475.

49. C.-Y. Chen, H.-W. Chang, Y.-F. Chang, B.-J. Chang, Y.-S. Lin, P.-S. Jian, H.-C. Yeh, H.-T. Chien, E.-C. Chen, Y.-C. Chao, H.-F. Meng, H.-W. Zan, H.-W. Lin, S.-F. Horng, Y.-J. Cheng, F.-W. Yen, I.-F. Lin, H.-Y. Yang, K.-J. Huang, and M.-R. Tseng, *J. Appl. Phys.*, 2011, **110**, 094501.

50. P. Schilinsky, C. Waldauf, and C. J. Brabec, *Adv. Funct. Mater.*, 2006, **16**, 1669–1672.

51. C. Lungenschmied, G. Dennler, H. Neugebauer, S. N. Sariciftci, M. Glatthaar, T. Meyer, and A. Meyer, *Sol. Energy Mater. Sol. Cells*, 2007, **91**, 379–384.

52. F. Padinger, C. J. Brabec, T. Fromherz, and J. C. Hummelen, *Opto-Electronics Rev.*, 2000, **8**, 280–283.

53. N. Shin, L. J. Richter, A. A. Herzing, R. J. Kline, and D. M. DeLongchamp, *Adv. Energy Mater.*, 2013, **3**, 938–948.

54. U. Aygül, D. Batchelor, U. Dettinger, S. Yilmaz, S. Allard, U. Scherf, H. Peisert, and T. Chassé, *J. Phys. Chem. C*, 2012, **116**, 4870–4874.

55. B. Schmidt-Hansberg, M. Sanyal, M. F. G. Klein, M. Pfaff, N. Schnabel, S. Jaiser, A. Vorobiev, E. Müller, A. Colsmann, P. Scharfer, D. Gerthsen, U. Lemmer, E. Barrena, and W. Schabel, *ACS Nano*, 2011, **5**, 8579–90.

56. W.-B. Byun, S. K. Lee, J.-C. Lee, S.-J. Moon, and W. S. Shin, *Curr. Appl. Phys.*, 2011, **11**, S179–S184.

57. Y.-H. Chang, S.-R. Tseng, C.-Y. Chen, H.-F. Meng, E.-C. Chen, S.-F. Horng, and C.-S. Hsu, *Org. Electron.*, 2009, **10**, 741–746.

58. J. Krantz, M. Richter, S. Spallek, E. Spiecker, and C. J. Brabec, *Adv. Funct. Mater.*, 2011, **21**, 4784–4787.

59. J.-S. Yu, G. H. Jung, J. Jo, J. S. Kim, J. W. Kim, S.-W. Kwak, J.-L. Lee, I. Kim, and D. Kim, *Sol. Energy Mater. Sol. Cells*, 2013, **109**, 142–147.

60. K.-H. Lee, B.-Y. Choi, J.-W. Park, S.-J. Kang, S.-M. Kim, D.-Y. Kim, and G.-Y. Jung, *Org. Electron.*, 2010, **11**, 748–754.

61. N. Li, D. Baran, K. Forberich, F. Machui, T. Ameri, M. Turbiez, M. Carrasco-Orozco, M. Drees, A. Facchetti, F. C. Krebs, and C. J. Brabec, *Energy Environ. Sci.*, 2013, **6**, 3407.

62. J. Ajuria, I. Etxebarria, W. Cambarau, U. Muñecas, R. Tena-Zaera, J. C. Jimeno, and R. Pacios, *Energy Environ. Sci.*, 2011, **4**, 453.

63. N. Li, D. Baran, K. Forberich, M. Turbiez, T. Ameri, F. C. Krebs, and C. J. Brabec, *Adv. Energy Mater.*, 2013, **3**, 1597–1605.

64. F. Jakubka, M. Heyder, F. Machui, J. Kaschta, D. Eggerath, W. Lövenich, F. C. Krebs, and C. J. Brabec, *Sol. Energy Mater. Sol. Cells*, 2013, **109**, 120–125.

65. F. C. Krebs, *Sol. Energy Mater. Sol. Cells*, 2009, **93**, 394–412.

66. F. C. Krebs, S. A. Gevorgyan, and J. Alstrup, *J. Mater. Chem.*, 2009, **19**, 5442.

67. F. C. Krebs, Y. Thomann, R. Thomann, and J. W. Andreasen, *Nanotechnology*, 2008, **19**, 424013.

68. T. R. Andersen, T. T. Larsen-Olsen, B. Andreasen, A. P. L. Böttiger, J. E. Carlé, M. Helgesen, E. Bundgaard, K. Norrman, J. W. Andreasen, M. Jørgensen, and F. C. Krebs, *ACS Nano*, 2011, **5**, 4188–4196.

69. F. Machui, L. Lucera, G. D. Spyropoulos, J. Cordero, A. S. Ali, P. Kubis, T. Ameri, M. M. Voigt, and C. J. Brabec, *Sol. Energy Mater. Sol. Cells*, 2014, **128**, 441–446.

70. Y.-X. Nan, X.-L. Hu, T. T. Larsen-Olsen, B. Andreasen, T. Tromholt, J. W. Andreasen, D. M. Tanenbaum, H.-Z. Chen, and F. C. Krebs, *Nanotechnology*, 2011, **22**, 475301.

71. F. C. Krebs, J. Alstrup, H. Spanggaard, K. Larsen, and E. Kold, *Sol. Energy Mater. Sol. Cells*, 2004, **83**, 293–300.

72. N. Espinosa, F. O. Lenzmann, S. Ryley, D. Angmo, M. Hösel, R. R. Søndergaard, D. Huss, S. Dafinger, S. Gritsch, J. M. Kroon, M. Jørgensen, and F. C. Krebs, *J. Mater. Chem. A*, 2013, **1**, 7037.

73. S. Hong, J. Lee, H. Kang, and K. Lee, *Sol. Energy Mater. Sol. Cells*, 2013, **112**, 27–35.

74. F. C. Krebs, M. Jørgensen, K. Norrman, O. Hagemann, J. Alstrup, T. D. Nielsen, J. Fyenbo, K. Larsen, and J. Kristensen, *Sol. Energy Mater. Sol. Cells*, 2009, **93**, 422–441.